Diverse structural assemblies of silver-thiophene-2, 5-dicarboxylate coordination complexes contribute to different proton-conducting performances

Xiao-Feng Zheng*, Wen-Qiang Li, Jun Du, Xian-Zhu Luo, Miao-Miao Liu, Yang Yu and Lai-Jin Tian

School of Chemistry and Chemical Engineering, Qufu Normal University, Qufu 273165, PR China

* To whom correspondence should be addressed. E-mail: xiaofengzheng004@163.com.

Table S1. The corresponding physical quantities of complexes **1** - **3** and the polymer **1** / **2**-PVDF.

	L / cm	S / cm^2	R / Ω	σ / $S \cdot cm^{-1}$
Complex **1**	0.15	0.25	30.15	1.99×10^{-2}
Complex **2**	0.097	0.5	45.55	4.25×10^{-3}
Complex **3**	0.06	0.5	64.43	1.98×10^{-3}
Polymer **1**-PVDF	0.025	1.045	11.00	2.17×10^{-3}
Polymer **2**-PVDF	0.025	1.045	26.60	8.99×10^{-4}

Table S2. Selected Bond Lengths (Å) and Angles (deg) for Complex **1-3**[a]

		Complex **1**	
Ag1-O3	2.4150(18)	Ag1-P1	2.4328(7)
Ag1-P2	2.4496(7)	Ag1-O1	2.4743(18)
O3-Ag1-P1	106.37(5)	O3-Ag1-P2	103.13(5)
P1-Ag1-P2	143.83(2)	O3-Ag1-O1	93.18(7)
P1-Ag1-O1	105.71(5)	P2-Ag1-O1	92.96(5)
		Complex **2**	
Ag1-N1	2.155(3)	Ag2-O3	2.240(4)
Ag1-O1	2.168(3)	Ag2-N3	2.345(4)
$Ag1-O1^{i}$	2.482(3)	$Ag2-O4^{ii}$	2.189(4)
$Ag2-Ag2^{ii}$	2.8923(12)		
N1-Ag1-O1	155.43(12)	$N1-Ag1-O1^{i}$	97.56(12)
$O1-Ag1-O1^{i}$	104.76(6)	$O4^{ii}$-Ag2-O3	159.76(16)
$O4^{ii}$-Ag2-N3	104.83(16)	O3-Ag2-N3	95.27(15)
$O4^{ii}$-Ag2- $Ag2^{ii}$	81.44(13)	O3-Ag2- $Ag2^{ii}$	80.78(12)
N3-Ag2- $Ag2^{ii}$	157.87(11)	$Ag1-O1-Ag1^{i}$	117.91(12)
		Complex **3**	
Ag1-N4	2.356(2)	Ag1-N2	2.485(3)

Ag1-O1	2.471(3)	Ag1-N1	2.504(3)
Ag2-O4	2.326(3)	Ag2-N8	2.355(3)
Ag2-N5	2.363(3)	Ag2-O3	2.495(3)
Ag2-Ag2^{ii}	3.4145(5)		
N4-Ag1-O1	129.72(8)	N4-Ag1-N2	111.95(9)
O1-Ag1-N2	79.61(8)	N4-Ag1-N1	117.26(9)
O1-Ag1-N1	83.55(8)	N2-Ag1-N1	127.13(8)
O4-Ag2-N8	108.62(13)	O4-Ag2-N5	112.00(11)
N8-Ag2-N5	115.38(10)	O4-Ag2-O3	111.95(11)
N8-Ag2-O3	90.96(12)	N5-Ag2-O3	116.14(11)

[a] Symmetry codes for **2:** i, 1-x, -1/2+y, 2-z; ii, 1-x, 1/2+y, 2-z; iii, 1-x, 2-y, 2-z; **3**: i, 1-x, -1/2+y, 2-z; ii, 1-x, 1/2+y, 2-z; iii, 1-x, 2-y, 2-z.

Table S3. H-Bonding Geometry Parameters (Å and deg) for Complex **2**[a]

D-H···O	D-H	H···O	D···A	D-H···A
		Complex **2**		
N2-H2B···O2^{i}	0.89	2.37	2.964(4)	124
		Complex **3**		
O(5)-H(5A)···O(7)	0.85	2.17	2.995(5)	166
O(5)-H(5B)···O(3)i	0.85	2.15	2.939(5)	155
O(6)-H(6A)···O(1)	0.85	1.90	2.735(3)	168
O(6)-H(6B)···N(7)ii	0.85	2.06	2.910(4)	177
O(7)-H(7A)···O(2)i	0.85	2.07	2.885(3)	161
O(7)-H(7B)···O(6)iii	0.85	1.95	2.794(3)	173

[a] Symmetry codes for **2**: i, -1+x, y, z; ii, 3/2-x,1/2+y,z; iii, 1/2-x,1/2+y,z; **3**: i, 2-x, -1/2+y, 1/2-z.

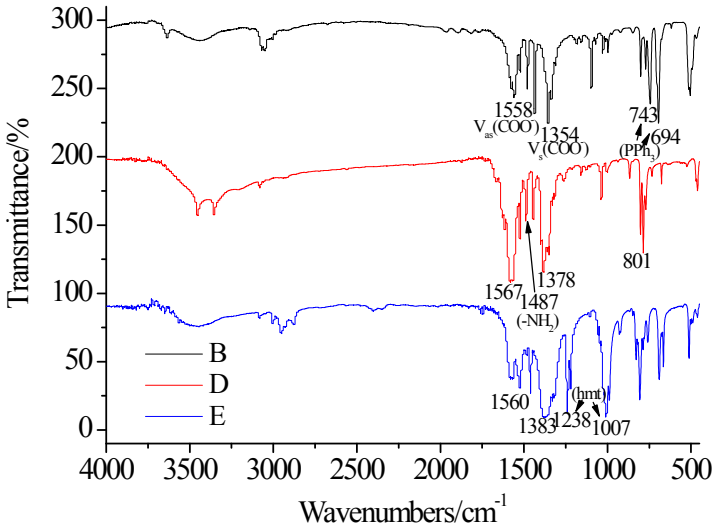

Figure S1, FT-IR spectra of **1** - **3** respectively.

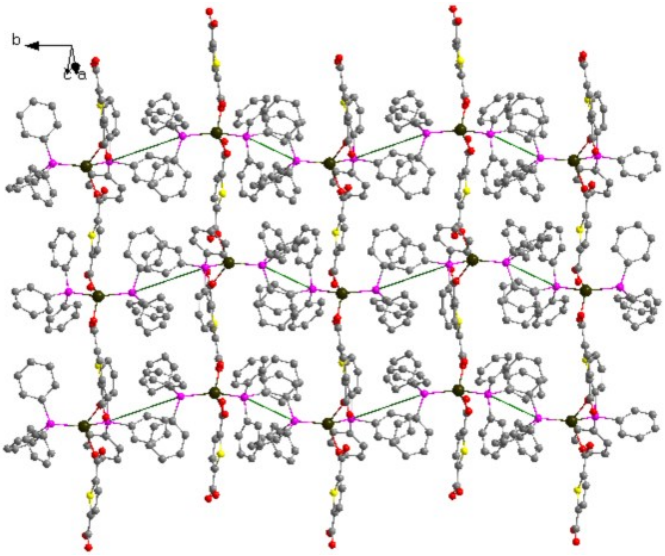

Figure S2, The 2-D layer formed by 4PE (the green robs) motifs between the 1-D chains in **1**. The H atoms are omitted for clearity.

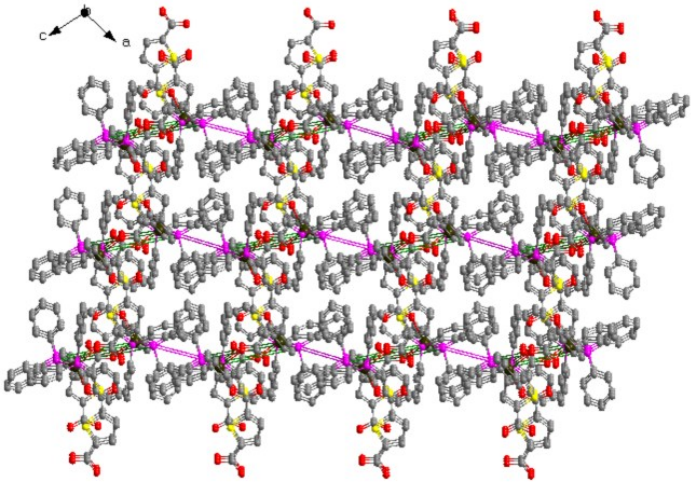

Figure S3, The 3-D network formed by 6PE (the brown robs) and 4PE (the green robs) motifs between the 2-D layers in **1**. The H atoms are omitted for clearity.

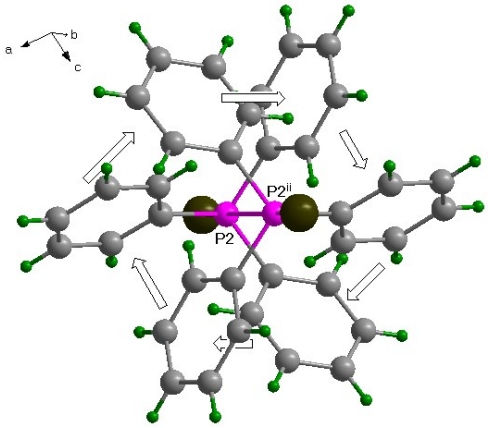

Figure S4, The pseudo-ideal weak 6PE motif between two PPh_3 at P2: the torsion angles for the rings involved are 30, 33 and 57°(and -30, -33 and -57°). The 6PE is

centrosymmetric [at centres of inversion of type (0.5, 0, 0.5 – site 2c)], with a P…P distance of 7.13 Å; Symmetry codes: ii, 1-x, -y, 1-z.

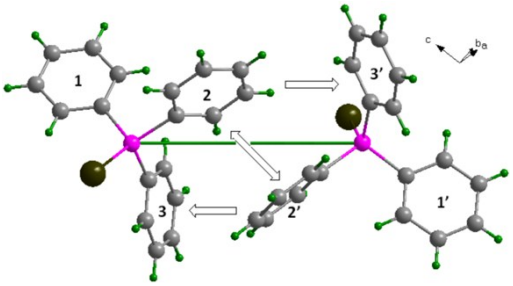

Figure S5, The pseudo weak 4PE motif: the torsion angles for the rings involved are 16 and -68° (84 and -63°), which is non-centrosymmetric with a P…P distance of 7.72 Å. The **off** interaction occurs between rings 2 and 2', while the interactions from 2→3' and 2' →3 are intermediate between **vf** and **ef**.

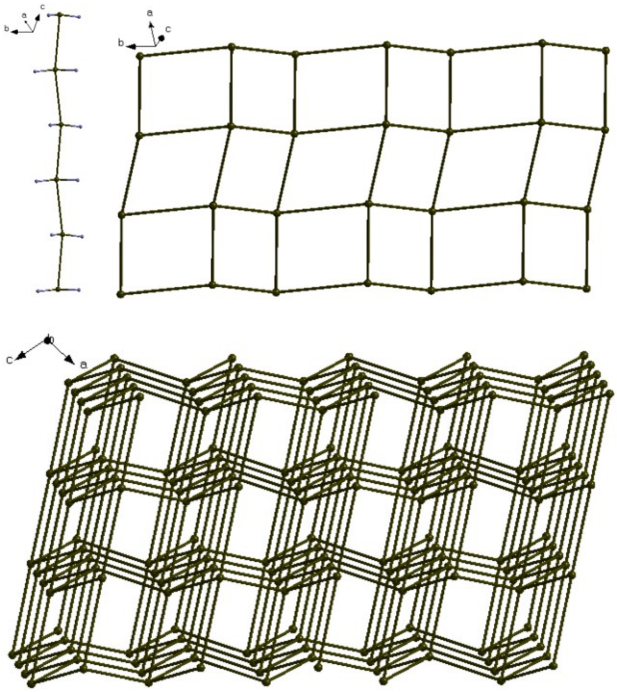

Figure S6, The schematic topological presentation for the structure of **1**.

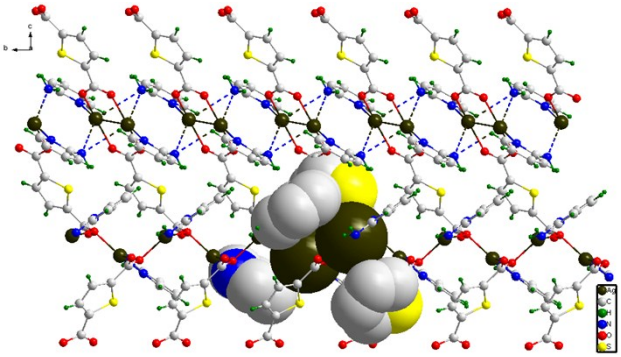

Figure S7, The Ag-π interactions and long Ag···N interactions in **2**. Parts of Ag-π interactions are pictured in space-filling modes.

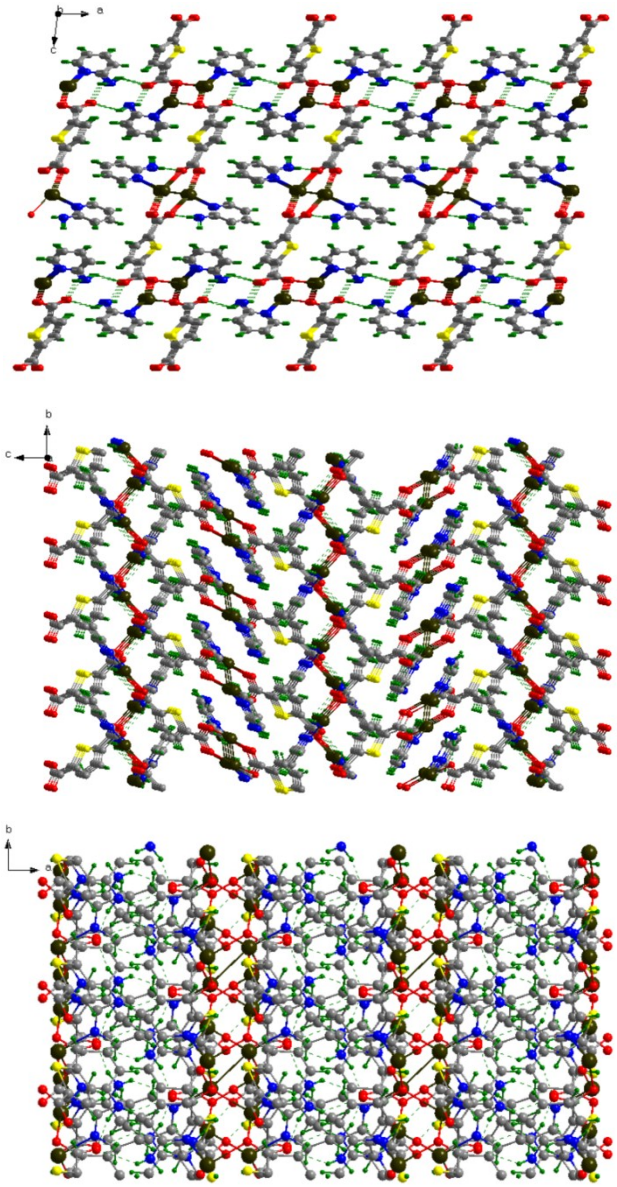

Figure S8, The 3D brick-wall network along b-axis in **2**.

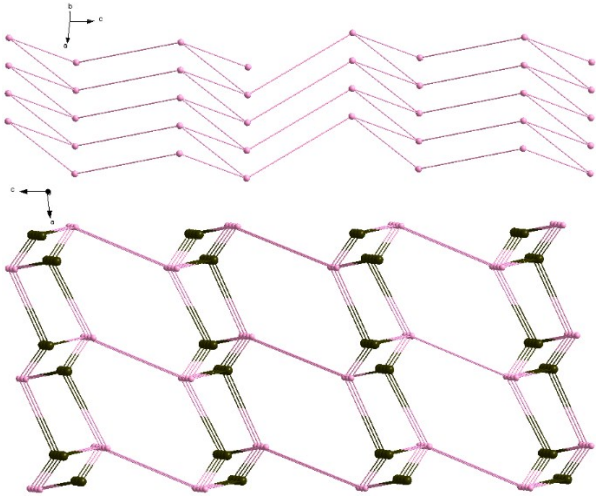

Figure S9, The schematic topological presentation for the structure of **2**.

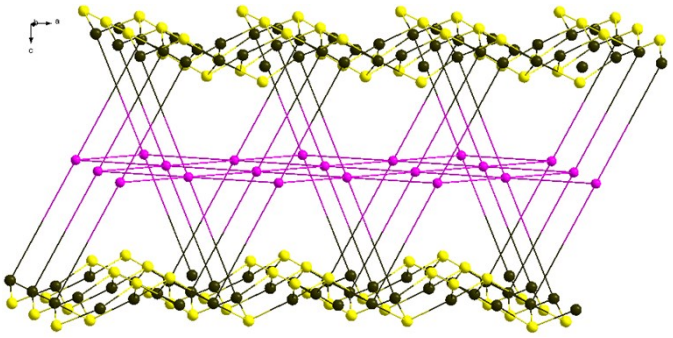

Figure S10, The schematic topological presentation for the structure of **3**.n

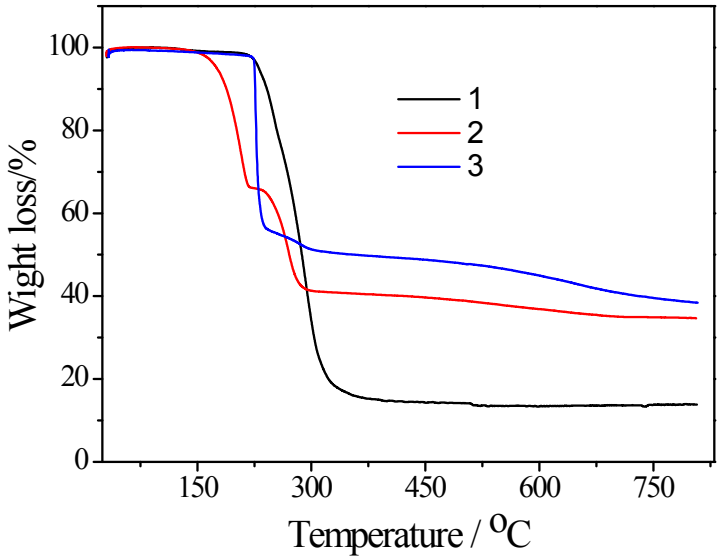

Figure S11, Thermogravimetric analysis (TGA) data for **1**-**3**.

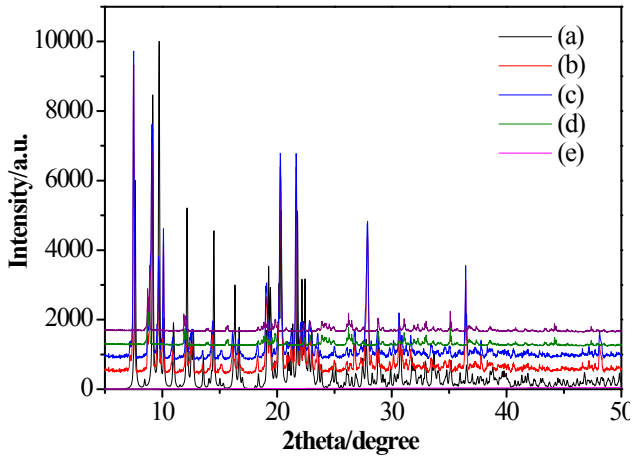

Figure S12, PXRD patterns showing the structural integrity in water of compound **1**. (a) Simulated PXRD patterns, (b) as-prepared of **1**, and after soaked in H_2O at r.t. for (c) 1 d, (d) 3 d, (e) 7 d.

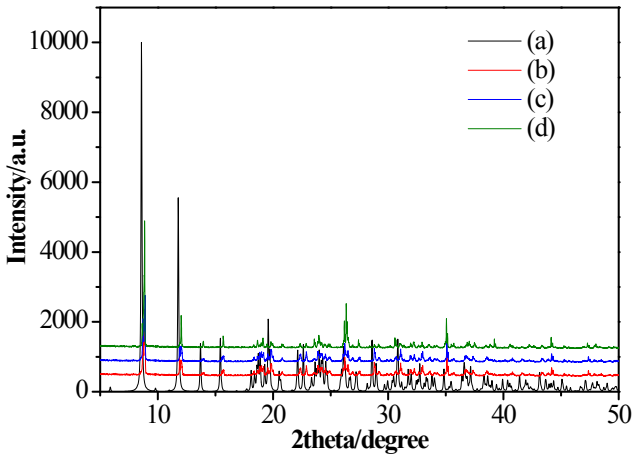

Figure S13, PXRD patterns showing the structural integrity in water of compound **2**. (a) Simulated PXRD patterns, (b) as-prepared of **2**, and after soaked in H_2O at r.t. for (c) 1 d, (d) 7 d.

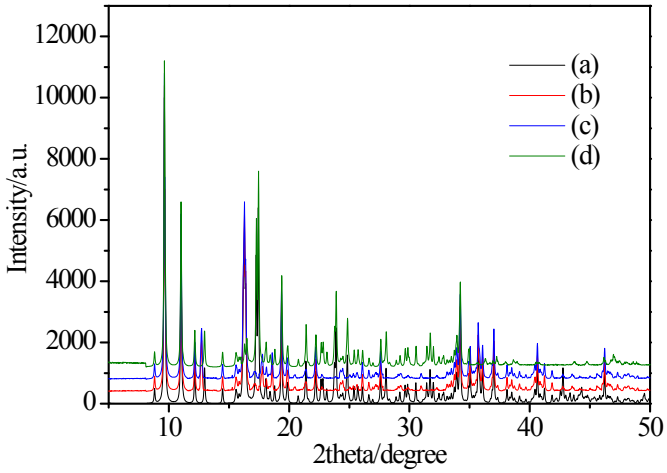

Figure S14, PXRD patterns showing the structural integrity in water of compound **3**. (a) Simulated PXRD patterns, (b) as-prepared of **3**, and after soaked in H_2O at r.t. for (c) 1 d, (d) 7 d.